

Integration of a field-effect-transistor terahertz detector with a diagonal horn antenna

Xiang Li(李想), Jian-dong Sun(孙建东), Zhi-peng Zhang(张志鹏), V V Popov, Hua Qin(秦华)
Citation: Chin. Phys. B . 2018, 27(6): 068506. **doi:** 10.1088/1674-1056/27/6/068506

Journal homepage: http://cpb.iphy.ac.cn; http://iopscience.iop.org/cpb

What follows is a list of articles you may be interested in

Mapping an on-chip terahertz antenna by a scanning near-field probe and a fixed field-effect transistor

Lü Li, Sun Jian-Dong, Roger A. Lewis, Sun Yun-Fei, Wu Dong-Min, Cai Yong, Qin Hua
Chin. Phys. B . 2015, 24(2): 028504. **doi:** 10.1088/1674-1056/24/2/028504

100-nm T-gate InAlAs/InGaAs InP-based HEMTs with f_T=249 GHz and f_{max}=415 GHz

Wang Li-Dan, Ding Peng, Su Yong-Bo, Chen Jiao, Zhang Bi-Chan, Jin Zhi
Chin. Phys. B . 2014, 23(3): 038501. **doi:** 10.1088/1674-1056/23/3/038501

0.15-μm T-gate $In_{0.52}Al_{0.48}As/In_{0.53}Ga_{0.47}As$ InP-based HEMT with f_{max} of 390 GHz

Zhong Ying-Hui, Zhang Yu-Ming, Zhang Yi-Men, Wang Xian-Tai, Lü Hong-Liang, Liu Xin-Yu, Jin Zhi
Chin. Phys. B . 2013, 22(12): 128503. **doi:** 10.1088/1674-1056/22/12/128503

AlGaN/GaN high-electron-mobility transistor with transparent gate by Al-doped ZnO

Wang Chong, He Yun-Long, Zheng Xue-Feng, Ma Xiao-Hua, Zhang Jin-Cheng, Hao Yue
Chin. Phys. B . 2013, 22(6): 068503. **doi:** 10.1088/1674-1056/22/6/068503

Enhancement of terahertz coupling efficiency by improved antenna design in GaN/AlGaN high electron mobility transistor detectors

Sun Yun-Fei, Sun Jan-Dong, Zhang Xiao-Yu, Qin Hua, Zhang Bao-Shun, Wu Dong-Min
Chin. Phys. B . 2012, 21(10): 108504. **doi:** 10.1088/1674-1056/21/10/108504

Integration of a field-effect-transistor terahertz detector with a diagonal horn antenna*

Xiang Li(李想)[1,2], Jian-dong Sun(孙建东)[2,†], Zhi-peng Zhang(张志鹏)[2], V V Popov[3], and Hua Qin(秦华)[2,‡]

[1] School of Nano Technology and Nano Bionics, University of Science and Technology of China, Hefei 230026, China
[2] Key Laboratory of Nanodevices and Applications, Suzhou Institute of Nano-tech and Nano-bionics, Chinese Academy of Sciences, Suzhou 215123, China
[3] Kotelnikov Institute of Radio Engineering and Electronics, Saratov Branch, Russian Academy of Sciences, Saratov 410019, Russia

(Received 25 December 2017; revised manuscript received 8 March 2018; published online 10 May 2018)

Efficient coupling of terahertz electromagnetic wave with the active region in a terahertz detector is required to enhance the optical sensitivity. In this work, we demonstrate direct integration of a field-effect-transistor (FET) terahertz detector chip at the waveguide port of a horn antenna. Although the integration without a proper backshot is rather preliminary, the noise-equivalent power is greatly reduced from 2.7 nW/Hz$^{1/2}$ for the bare detector chip to 76 pW/Hz$^{1/2}$ at 340 GHz. The enhancement factor of about 30 is confirmed by simulations revealing the effective increase in the energy flux density seen by the detector. The simulation further confirms the frequency response of the horn antenna and the on-chip antennas. A design with the detector chip fully embedded within a waveguide cavity could be made to further enhance the coupling efficiency.

Keywords: terahertz detector, high electron mobility transistor, diagonal horn

PACS: 85.60.Gz, 72.80.Ey, 42.82.Et, 87.50.U– **DOI:** 10.1088/1674-1056/27/6/068506

1. Introduction

The sensitivity of a detector module for sensing an electromagnetic wave is determined not only by the inherent 'electrical' sensitivity of the implemented detector chip but also by the coupling efficiency between the incident energy flux and the detector chip. When the latter is considered, the sensitivity is termed as 'optical' sensitivity. Optical coupling becomes more important in the terahertz frequency band than that in the infrared or visible regimes since the dimension of the active region of a terahertz detector is usually smaller than or comparable with the wavelength. In the terahertz regime, an on-chip terahertz antenna/probe is commonly integrated with the detector so that the terahertz electromagnetic wave could be coupled to the active detector region.[1–5] Efficient coupling between the terahertz electromagnetic wave in free space and the terahertz antenna/probe is realized either by using a waveguide structure or by using a silicon lens.[6,7] The waveguide-based solution offers a higher coupling efficiency while the lens-based 'quasi-optical' coupling scheme offers a wider bandwidth.[8–10] For example, a Schottky-barrier-diode (SBD) detector can be found in waveguide-coupled or lens-coupled modules, which are now commercially available. Note that the NEP can be further reduced by reducing both the gate length and the gap between the gate and the antennas down to 200 nm, and the NEP integrated silicon lens could be below 10 pW/Hz$^{1/2}$. An extended report on this approach will be prepared for publication elsewhere. Waveguide-coupled SBD detectors are of the main-stream solution for frequency below 1 THz and the lens-based 'quasi-optical' solution is more appropriate for wideband applications.[11,12] A typical lens-coupled SBD detector can offer an 'optical' sensitivity of around 10 pW/Hz$^{1/2}$ while the optical sensitivity of the waveguide-coupled SBD detector is usually less than 10 pW/Hz$^{1/2}$.[5]

In comparison with the relatively well-developed SBD detectors, burgeoning field-effect-transistor (FET) detectors are expected to have a higher sensitivity, wider response spectrum, and technical feasibility in making large detector arrays. A silicon-lens-coupled FET terahertz detector has achieved an optical sensitivity of less than 10 pW/Hz$^{1/2}$ at 630 GHz,[13] being close to that of waveguide-coupled SBD detectors. Waveguide-coupled FET gets preliminary attempted, like the coplanar waveguide is used in the process of the signal transmission of FET,[14] while no direct integration of FET detectors with spatial waveguide structure has been reported so far. It is thus an interesting question to answer if a waveguide-coupled FET detector could be made or if such integration could offer a higher sensitivity than lens-coupled FET de-

*Project supported by the National Key Research and Development Program of China (Grant Nos. 2016YFF0100501 and 2016YFC0801203), the National Natural Science Foundation of China (Grant Nos. 61611530708, 11403084, 61401456, 61401297, and 61505242), the Six Talent Peaks Project of Jiangsu Province, China (Grant No. XXRJ-079), the Youth Innovation Promotion Association of Chinese Academy of Sciences (Grant No. 2017372), and the Russian Foundation for Basic Research (Grant No. 17-52-53063).

†Corresponding author. E-mail: jdsun2008@sinano.ac.cn
‡Corresponding author. E-mail: hqin2007@sinano.ac.cn

© 2018 Chinese Physical Society and IOP Publishing Ltd

tectors or waveguide-coupled SBD detectors. Here, we report our attempt in directly integrating an AlGaN/GaN FET detector with a diagonal horn[15] antenna. Although the integration is rather straightforward by attaching the detector chip right at the waveguide port, a gain of 14.8 dB has been obtained and the proof-of-concept indicates that the integration/coupling could be further optimized.

2. Experimental setup

A diagonal horn antenna consisting of a rectangular waveguide part and a diagonal horn is used to couple an incident terahertz electromagnetic wave to a detector chip attached at the exit of the waveguide, as shown in Figs. 1(a) and 1(b). The diagonal horn has a total length of 13 mm, a waveguide port of 560 μm × 280 μm, and is designed for 340 GHz. The detector chip directly attached at the waveguide exit is wired to a printed circuit board so that the source is connected to the ground, a gate voltage V_G is applied, and the detector signal is sent to a low-noise current preamplifier. The details of the detector and its location relative to the rectangular waveguide port are shown in Fig. 1(c). The detector is one out of the two detectors in a differential configuration as has been reported in our previous work.[16] The detectors are made on an AlGaN/GaN heterostructure with a sapphire substrate.[17] For a single detector, three antennas named as the d-antenna, s-antenna, and g-antenna are the key elements for manipulating the terahertz electromagnetic wave in the gated two-dimensional electron gas (2DEG) formed in the AlGaN/GaN heterostructure under the gate which is directly connected with the g-antenna.[18] The d-antenna and the s-antenna are placed on top of the 2DEG mesa for the drain and the source electrodes, respectively. It can be seen that the detector body is placed very close to the center of the rectangular waveguide port and the detector is fully enclosed within the rectangular port. The antennnas are placed in direction x so that they couple well with the waveguide modes.

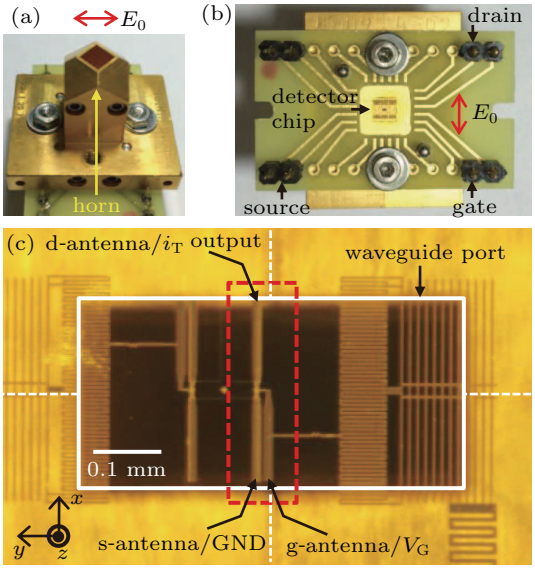


Fig. 1. (color online) (a) Overview of the horn antenna integrated with a detector chip. (b) Assembling of the detector chip at the waveguide exit of the horn antenna. (c) Zoom-in view of the detector chip placed at the center of the waveguide port. The dashed lines mark the center of the waveguide port.

3. Results and discussion

The 'optical' sensitivity, represented by the noise-equivalent power (NEP), considers the incident power within the diagonal horn. The overall response of the detector to the incident terahertz electromagnetic wave depends not only on the field distribution at the waveguide port but also on the on-chip antennas as shown in Fig. 1(c). It is the on-chip antenna that couples the terahertz electromagnetic wave into the active region, i.e., 2DEG controlled by the gate. The asymmetric distribution of the energy flux across the gated electron channel plays the key role in generating the terahertz photocurrent.[17] The effect of such antenna-coupled field-effect transistor can be well described by the self-mixing model and has been reported in depth in our previous publications.[16–19] According to the self-mixing model, the photocurrent (i_T) is proportional to the product of the field-effect factor dn/dV_G and the on-chip-antenna factor Λ, which can be expressed as

$$\Lambda = \int_0^L \dot{\xi}_x \dot{\xi}_z \cos\phi \, dx, \tag{1}$$

with L the length of the channel, $\dot{\xi}_x = d\xi_x/dx$, $\dot{\xi}_z = d\xi_z/dz$, and ϕ the horizontal and perpendicular terahertz field enhancement factors, and the phase difference in between, respectively.

Prior to the integration, simulations are performed to reveal the energy flux within the horn antenna and its waveguide. To evaluate the coupling coefficient, the horn-antenna factor (F_H) is defined as the ratio of the energy flux (J_0) at the center of the detector location to that at the input port of the horn antenna. As shown in Figs. 2(a) and 2(b), the effective beam size is reduced from millimeter size to the dimension of the waveguide port. About 79.6 % of the energy flux at the waveguide port is concentrated within the effective area of the detector, which is about $\lambda^2/8$ where λ is the wavelength at 340 GHz. In comparison, as shown in Fig. 2(c), the terahertz beam spot at the focal point of a 3″ off-axis parabolic (OAP) mirror mapped by using a similar detector without horn antenna is found to have a beam radius of 1.3 mm. In this case, only 2.3% of the energy flux can be received by the detector. It is thus clear that the detector integrated with a horn antenna is coupled to the terahertz electromagnetic wave with a much higher efficiency than the bare detector coupling to the focused terahertz beam by an OAP mirror. Further simulations by taking into account the on-chip antenna and the horn

antenna gives the antenna factor respectively at various frequencies from 100 GHz to 500 GHz, as shown in Fig. 2(d). As expected, the horn antenna factor exhibits a cut-off frequency about 268 GHz determined by the rectangular waveguide. A maximum factor about 40 at 307 GHz is obtained and the factor reduces to 20 when the frequency increases to 440 GHz, and the simulated on-chip antenna factor as a function of the frequency has a maximum in the band of the horn antenna.

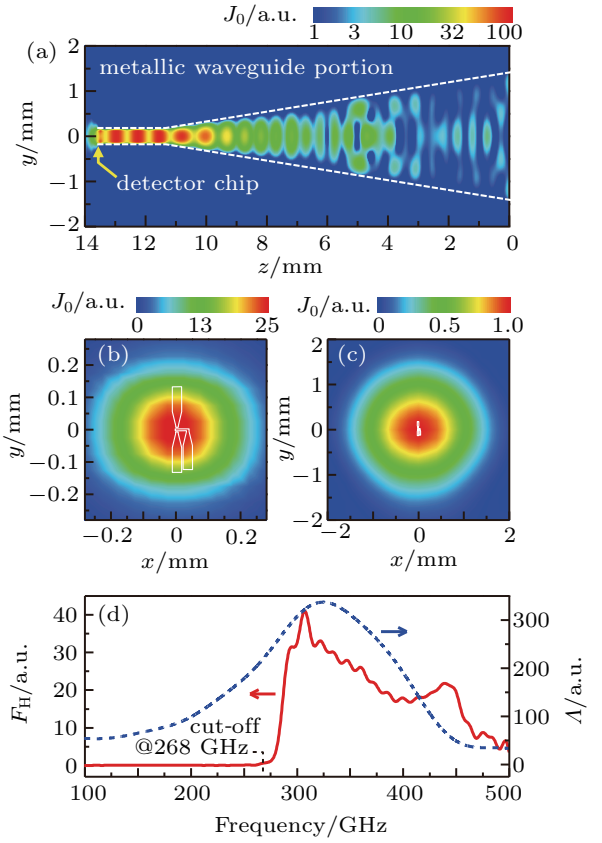


Fig. 2. (color online) (a) Overview of the simulated energy flux density (J_0) in the horn antenna at 340 GHz. (b) Simulated energy flux density at the waveguide port of the diagonal horn at 340 GHz. (c) Experimental energy flux density of the terahertz beam at 340 GHz focused by a 3″ off-axis parabolic mirror. (d) Simulated horn-antenna factor (F_H) and on-chip-antenna factor (Λ) as a function of the frequency. The unit a.u. is short for arbtrary units.

Since the gate voltage is fixed at the optimal value ($V_G = -3.1$ V) to maximize the photoresponse, the detector response as a function of the frequency reflects directly the terahertz energy flux seen by the detector and hence the overall antenna factor F_O, which is the product of the horn-antenna factor and on-chip-antenna factor ($F_O = F_H \times \Lambda$). A combined simulation considering both the on-chip-antenna and the waveguide would require a large computation power, which is not available in our lab.

The terahertz photocurrent from the integrated detector is compared with that from the bare detector, as shown in Fig. 3(a). An enhancement of about 30 is obtained from 290 GHz to 360 GHz and agrees well with the simulated horn antenna factor shown in Fig. 2(d). As shown in Fig. 3(b), the integrated detector now offers a noise-equivalent power (NEP) about 76 pW/Hz$^{1/2}$ at 340 GHz, which is otherwise about 2.7 nW/Hz$^{1/2}$ for the bare detector, agrees with the enhancement factor of about 30. With frequency below 268 GHz, i.e., in the stop band of the waveguide, the photocurrent is strongly suppressed. The responsivity of the integrated detector from 200 GHz to 380 GHz shown in Fig. 3(c) agrees with the simulated overall antenna factor, which is the product of the simulated horn-antenna factor and on-chip-antenna factor as shown in Fig. 2(d). To validate the sensitive response for terahertz imaging applications, the integrated detector is used to sense the transmitted terahertz power at 340 GHz through a fresh leaf, which is raster scanned at the confocal point of a pair of 3″ OAPs. As shown in Fig. 4, the spatial resolution is about 0.2 mm.

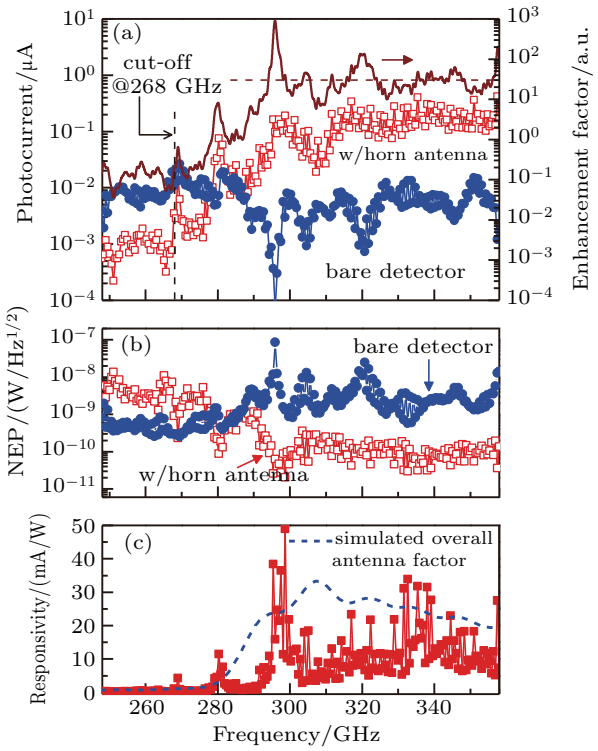


Fig. 3. (color online) (a) Terahertz photocurrent from the integrated detector and the bare detector. The enhancement factor for the integrated detector is plotted to the right axis. (b) Noise-equivalent power (NEP) for the same detector with and without the horn antenna integrated. (c) Measured responsivity for the integrated detector in comparison with the simulated overall antenna factor (dashed curve).

The electrical sensitivity can be enhanced by reducing the gap between s-antenna and d-antenna and the length of gate. A FET detector with a 200-nm-long gate now can offer a NEP one order of magnitude lower than the current detector chip.[14] Hence, waveguide-coupled FET detectors with NEP below 1 pW/Hz$^{1/2}$ could be expected to surpass the waveguide-coupled SBD detectors. To this end, optimization on the detector design and integration has to be performed. For example, partially learned from waveguide-integrated SBD

detectors,[6] it is highly desired to have the detector chip fully encapsulated within a waveguide cavity so that the terahertz field strength could be maximized within a certain frequency band. In the current integration scheme, the open boundary at the detector surface induces reflection and hence interferences, which can be seen as those large variations in the responsivity shown in Fig. 3. Since FET-based detectors, being three-terminal, are different from the two-terminal SBD detectors, it requires more detailed design of the on-chip antennas as field probes in the waveguide and a proper impedance matching to the gate controlled channel.

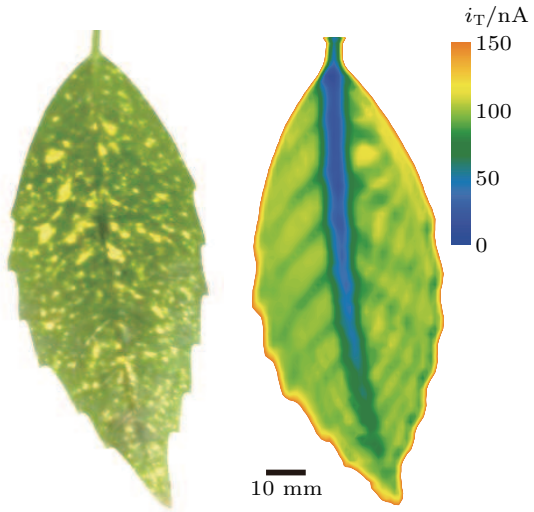


Fig. 4. (color online) Transmission raster-scan imaging (right) of a fresh leaf at 340 GHz and the optical counterpart (left).

4. Conclusion

In conclusion, we demonstrate the effective enhancement in responsivity/sensitivity of an FET-based terahertz detector directly integrated with a horn antenna. The effect of the terahertz mode defined by the rectangular waveguide factor is quantitatively verified. Our results indicate that a more realistic and sensitive waveguide-coupled FET detector could be made by fully integrating the detector chip within a waveguide cavity.

References

[1] Cai Y, Brener I, Lopata J, Wynn J, Pfeiffer L, Stark J B, Wu Q, Zhang X C and Federici J F 1998 *Appl. Phys. Lett.* **73** 444
[2] Kawano Y and Ishibashi K 2008 *Nat. Photon.* **2** 618
[3] Richards P L 1994 *J. Appl. Phys.* **76** 1
[4] Feng W, Zhang R and Cao J C 2015 *Acta Phys. Sin.* **64** 229501 (in Chinese)
[5] See https://vadiodes.com/en/products/detectors for the specifications of different SBD detectors coupling with waveguide or silicon lens
[6] Ohkawa K, Sakakibara K, Aoki Y, Kikuma N and Hirayama H 2006 *Asia-Pacific Microwave Conference,* 2006*, APMC* 2006*, IEEE* p. 1837
[7] Kroug M, Cherednichenko S, Merkel H, Kollbergl E, Voronov B, Gol'tsman G, Huebers H W and Richter H 2001 *IEEE Trans. Appl. Supercond.* **11** 962
[8] Bowers J E and Burrus C A 1986 *Electron. Lett.* **22** 905
[9] Seliuta D, Kašalynas I, Tamošiūnas V, Balakauskas S, Martūnas Z, Ašmontas S, Valušis G, Lisauskas A, Roskos H G and Köhler K 2006 *Electron. Lett.* **42** 825
[10] Hadi R l, Sherry H, Grzyb J, Baktash N, Zhao Y, Ojefors E, Kaiser A, Cathelin A and Pfeiffer U, 2011 *Microwave Symposium Digest (MTT),* 2011 *IEEE* 1
[11] Hesler J L. and Crowe T W 2007 *ISSTT* 89
[12] Schoenherr D, Bleasdale C, Goebel T, Sydlo C, Hartnagel H L, Lewis R and Meissner P 2010 *35th International Conference on Infrared Millimeter and Terahertz Waves (IRMMW-THz), IEEE* 1
[13] Bauer M, Boppel S, Zhang J S, Rämer A, Chevtchenko S, Lisauskas A, Heinrich W, Krozer V and Roskos H G 2016 *International Journal of High Speed Electronics and Systems* **25** 1640013
[14] Andersson M A, Zhang Y X and Stake J 2017 *IEEE Trans. Microwave Theory Techniq.* **65** 165
[15] Johansson J F and Whyborn N D 1992 *IEEE Trans. Microwave Theory Techniq.* **40** 795
[16] Qin H, Li X, Sun J D, Zhang Z P, Sun Y F, Yu Y, Li X X and Luo M C 2017 *Appl. Phys. Lett.* **110** 171109
[17] Sun J D, Sun Y F, Wu D M, Cai Y, Qin H and Zhang B S 2012 *Appl. Phys. Lett.* **100** 013506
[18] Sun Y F, Sun J D, Zhang X Y, Qin H, Zhang B S and Wu D M 2012 *Chin. Phys. B* **21** 108504
[19] Yang X X, Sun J D, Qin H, Lv L, Su L N, Yan B, Li X X, Zhang Z P and Fang J Y 2015 *Chin. Phys. B* **24** 047206